EPJ Web of Conferences **2**, 13001 (2010)
DOI:10.1051/epjconf/20100213001

Excitation of compound states in the subsystems as indirect tool in nuclear astrophysics

A.M. Mukhamedzhanov[1,a], M. La Cognata[2], C. Spitaleri[2], and R. E. Tribble[1]

[1] Cyclotron Institute, Texas A&M University, College Station, Texas, USA
[2] DMFCI, Università di Catania, Catania, Italy and INFN-Laboratori Nazionali del Sud, Catania, Italy

Abstract. Astrophysical reactions proceeding through compound states represent one of the crucial part of nuclear astrophysics. However, due to the presence of the Coulomb barrier, it is often very difficult or even impossible to obtain the astrophysical $S(E)$ factor from measurements in the laboratory at astrophysically relevant energies. The Trojan Horse method (THM) provides a unique tool to obtain the information about resonant astrophysical reactions at astrophysically relevant energies. Here the theory and application of the THM for the resonant reactions is addressed.

1 Physics of the Trojan Horse method or why and how it works

Here, we describe the physics of the THM which explains why this method works. The THM, first suggested by Baur [1] and significantly modified by Spitaleri [2] to make it workable, involves obtaining the cross section of the binary process

$$x + A \to b + B \tag{1}$$

at astrophysical energies by measuring the Trojan Horse (TH) reaction (the two-body to the three-body process ($2 \to 3$))

$$a + A \to y + b + B, \tag{2}$$

in the quasi-free (QF) kinematics regime.

(i) The primary goal of the THM is to determine the astrophysical factor for rearrangement reactions at astrophysically relevant energies, at which direct measurements are impossible due to the very low cross section or distorted by the electron screening. To measure the cross section at astrophysical energies one has to overcome the Coulomb barrier in the initial channel of the binary reaction. In the THM it is achieved by using the TH particle $a = (y\,x)$, which contains one of the initial nuclei, x, of the binary reaction (1). Thus in the THM in the initial channel one uses $a = (y\,x) + A$ rather than $x + A$. The price we pay for this is the presence of three particles in the final state of the TH reaction, $y + b + B$, rather than the two-particle final state $b + B$ in the binary reaction. To increase the TH triple differential cross section the relative kinetic energy E_{Aa} in the initial channel of the TH reaction should be higher then the Coulomb barrier between particles A and a. Then the probability to find nucleus A near a is not suppressed by the Coulomb barrier, i.e. there is a finite probability that A can be in the proximity of x. It means that there is no additional Coulomb barrier between A and the constituent particle x of the TH nucleus a. Usually in literature the TH process is described as follows: the projectile a (or A), which is accelerated to an energy above the Coulomb barrier V_{Aa}^{CB}, approaches A (or a) and then breaks down in the vicinity of A. Particle x then remains interacting with A while y leaves the scene as a spectator.
(ii) To make this mechanism workable two additional conditions should be fulfilled. First, the QF kinematics (the relative momentum of y and x $p_{yx} = 0$) should be chosen. It provides the best condition to treat y as the spectator because it minimizes the interaction between y and x by favoring the maximal distances between these particles. In addition, the initial relative momentum k_{aA} should be large enough (typically $k_{aA} > \kappa_{yx}^{a}$), so that A will probe distances smaller than the distances between y and x available in the QF kinematics. Here $\kappa_{yx}^{a} = \sqrt{2\,\mu_{yx}\,\varepsilon_{yx}^{a}}$, μ_{yx} is the reduced mass of particles y and x, and ε_{yx}^{a} is the binding energy for the virtual decay $a \to y + x$.
(iii) Assuming that the TH reaction mechanism is described by the pole diagram, Fig. 1(a) from [3] (we use here a different notation for the final-state nuclei, y, b and B rather than s, c and C used in [3]). Then from the energy and momentum conservation in the three- and four-ray vertices of the pole diagram we get the basic equation of the TH reaction:

$$E_{Ax} = \frac{p_{Ax}^2}{2\,\mu_{Ax}} - \frac{p_{yx}^2}{2\,\mu_{yx}} - \varepsilon_{yx}^{a}, \tag{3}$$

where E_{ix} and $\mathbf{p}_{ix}$ are the relative kinetic energy and momentum of i and x. In the QF kinematics ($p_{yx} = 0$) it reduces to $E_{Ax} = \frac{p_{Ax}^2}{2\,\mu_{Ax}} - \varepsilon_{yx}^{a}$. Thus in the THM always $p_{Ax}^2/(2\,\mu_{Ax}) > E_{Ax}$. We also can conclude that the binding energy of the TH nucleus a compensates for the relative motion x and A making available low and even negative relative energy E_{Ax}.

[a] e-mail: akram@comp.tamu.edu

Here we need to add one more important comment. In the QF kinematics there is an unique correspondence between the incident energy E_A of nucleus A and E_{Ax}. It means that, to cover a finite E_{Ax} energy interval, the TH experiments should be performed at different accelerator energies, what practically is hardly feasible. That is why the TH experiments were performed at fixed projectile energy E_A but the spectator momentum was allowed to change in an interval $p_{yx} < \kappa^a_{yx}$. It allows one to cover enough interval in E_{xA} from astrophysically relevant energies up to energies where direct data are available. These higher energies are needed to normalize the TH astrophysical factor to the direct one.

(iv) There are two important tests of the THM. In the majority of the previous THM papers, see [4] and references therein, the plane wave impulse approximation (PWIA) was used. Comparison of the experimental momentum distribution of the spectator with the momentum distribution of the spectator in a free TH particle a provides the test of the PWIA. In a more accurate approach the initial and final state interactions in the TH reaction should be taken into account.

The second important test of the THM is comparison of the angular distribution of the fragments b and B measured in the TH reaction with the angular distribution of these fragments in the binary reaction (1). This test becomes especially important for resonant binary reactions [5].

(iiv) It is instructive to compare the QF kinematics with the kinematics of a standard stripping reaction to a bound state. It will help us to elucidate the difference between the QF kinematics employed in the THM and the conventional stripping process. To this end, let us compare the stripping $A(d,n)F$ reaction in the QF and conventional kinematics. Assume, for simplicity, that $m_A >> m_d$, where m_i is the mass of particle i.

Then in the QF kinematics, $p_{np} = 0$, $\mathbf{p}_p = -\mathbf{k}_n$ and the momentum of the neutron $k_n = \frac{k_d}{2}$. The energy conservation in the center of mass (c. m.) of the stripping reaction is ($k_{dA} = k_d$ and $k_{nF} = k_n$, $\mathbf{k}_i$ is the momentum of particle i)

$$\frac{k_d^2}{2\,\mu_{A\,d}} + Q = \frac{k_n^2}{2\,\mu_{F\,n}}, \tag{4}$$

we get that in the QF kinematics $E_{A\,d} \approx -2\,Q$. Thus the QF kinematics can be achieved only for endothermic reactions, which are stripping to unbound states or loosely bound states, $\varepsilon^a_{yx} > \varepsilon^F_{Ax}$. Note that for the stripping to the bound state $Q = \varepsilon^F_{Ap} - \varepsilon^d_{np}$ and for the stripping to the unbound state $Q = -E_{Ap} - \varepsilon^d_{np}$. In the QF kinematics the stripping probes the distances between the nucleons $r_{np} > 1/\kappa^d_{np}$, i.e. the nucleons in the deuteron are uncorrelated during the stripping and the angular distribution of the neutron-spectator is forward-peaked independently on the value of the orbital angular momentum of the resonance state in F, which is populated by the transferred proton.

To consider the classical stripping to the bound state, we assume, for simplicity, that $E_{Ad} >> |Q|$ and $m_A >> m_d$. Then from Eq. (4) we get $k_n = \frac{k_d}{\sqrt{2}}$. Thus the spectator momentum is higher by a factor of $\sqrt{2}$ than the one in the QF kinematics. Hence, the relative momentum of the nucleons in the deuteron can be large enough ($p_{np} > \kappa^d_{np}$) to probe small distances $r_{np} < 1/\kappa^d_{np}$, i.e. the nucleons in the deuteron in the classical stripping to the bound state can be correlated.

From $\mathbf{k}_d = \mathbf{k}_n + \mathbf{p}_p$ and the requirement that $p_p R \sim l_{Ap}$, where p_p is the momentum of the transferred proton, l_{Ap} is the orbital angular momentum of the proton bound state in the final nucleus $B = (Ap)$ and R is the radius of B, we find that the angle of the exiting neutron may depend on l_{Ap}: the larger l_B, the larger the angle. That is why the classical stripping to bound states was used and is being used (for exotic nuclei) as one of the major spectroscopic tools to determine the orbital angular momentum of the bound state.

2 Trojan Horse method for resonance reactions

Astrophysical reactions proceeding through compound states represent one of the crucial part of nuclear astrophysics. The THM provides a unique tool to obtain the information about resonant astrophysical reactions at astrophysically relevant energies due to the absence of the Coulomb barrier in the sub-system $A + x$. Let us consider the resonant reaction $A + x \to F \to B + b$. Its cross section is given by

$$\sigma(E_{Ax}) = \frac{\pi}{k^2_{Ax}}\,\frac{\hat{J}_F}{\hat{J}_A\,\hat{J}_x}\,\frac{\Gamma_{Bb}(E_{Bb})\,\Gamma_{Ax}(E_{Ax})}{(E_{Bb}-E_R)^2 + \frac{\Gamma^2(E_{Bb})}{4}}$$
$$\sim \frac{1}{k^2_{Ax}}\,P_{l_i}(E_{Ax}, r_{0(Ax)})\,P_{l_f}(E_{Bb}, r_{0(Bb)}), \tag{5}$$

where $\hat{J}_i = 2\,J_i + 1$, J_i is the spin of nucleus i.

We note that such an expression appears in the R matrix approach, where, in contrast to the Breit-Wigner expression, the resonance widths depend on the energy. Here, $\Gamma_{ij}(E_{ij})$ is the partial resonance width in the channel $i + j$, $\Gamma(E_{Bb}) = \Gamma_{Ax}(E_{Ax}) + \Gamma_{Bb}(E_{Bb})$ is the total resonance width and E_R is the real part of the resonance energy in the channel $B + b$.

We took into account that in the R matrix approach $\Gamma_{ij}(E_{ij}) = 2\,P_{l_{ij}}(E_{ij}, r_{0(ij)})\,\gamma^2_{ij}$, where $P_{l_{ij}}(E_{ij}, r_{0(ij)})$ is the barrier penetrability factor in the channel $i + j$ with relative orbital angular l_{ij}, which depends on E_{ij} and the channel radius $r_{0(ij)}$, and γ_{ij} is the observable partial reduced width in the channel $i + j$. This penetrability factor is the major obstacle to measure resonant cross sections at astrophysically relevant energies because at $E_{ij} \to 0$ $P_{l_{ij}}(E_{ij}, r_{0(ij)}) \sim exp(-2\,\pi\,\eta_{ij})$, where $\eta_{ij} = Z_i\,Z_j\,e^2\,\mu_{ij}/k_{ij}$ is the Coulomb parameter in the $i + j$ channel, $Z_i\,e$ is the charge of nucleus i. We use the system of units in which $\hbar = c = 1$.

The main advantage of the THM is that its triple differential cross section does not contain $P_{l_{Ax}}$. The TH double

differential cross section $\frac{\mathrm{d}^2\sigma^{TH}}{\mathrm{d}\Omega_{\hat{\mathbf{k}}_{yF}}\,\mathrm{d}E_{yF}}$ has a structure similar to the R matrix resonant cross section (5). The amplitude of the TH resonant reaction (2), which takes into account the $a+A$ scattering in the initial state and $y+F$ scattering in the intermediate state, is given by [6]

$$M^{TH}_{M_A\,M_a;M_y\,M_B\,M_b}(\mathbf{k}_{yF},\mathbf{k}_{Bb},\mathbf{k}_{Aa}) = \frac{\sum\limits_{M_F} M^{M_F}_{M_BM_b}(\mathbf{k}_{Bb})\,M_{M_yM_F;M_AM_a}(\mathbf{k}_{yF},\mathbf{k}_{Aa})}{E_{Bb}-E_R+i\frac{\Gamma(E_{Bb})}{2}} \tag{6}$$

and describes the two-step process. The amplitude $M_{M_yM_F;M_AM_a}$ corresponds to the first step, which is the transfer reaction $A(a,y)F$ populating the resonance state $F=A+x=B+b$.

The amplitude of the second step

$$M^{M_F}_{M_BM_b}(k_{Bb}) = \frac{2\pi}{\sqrt{\mu_{Bb}\,k_{Bb}}}\sum_{S_fM_{S_f}l_fm_{l_f}} < S_fM_{S_f}\,l_fm_{l_f}|J_FM_F >< J_B\,M_B\,J_b\,M_b|S_f\,M_{S_f} > [\Gamma_{Bb_{(S_fl_f)}}(E_{Bb})]^{1/2}e^{i\,\delta_{S_fl_f}}\,Y_{l_fm_{l_f}}(\hat{\mathbf{k}}_{Bb}) \tag{7}$$

corresponds the resonance decay $F\to B+b$, M_i is the projection of the spin J_i, S_f and M_{S_f} are the channel spin and its projection of the resonance in the exit channel $B+b$, $l_f=l_{Bb}$ and m_{l_f} are the relative orbital angular momentum and its projection of the fragments B and b in the resonance state F; $\mathbf{k}_{ij}$ is the relative momentum of the real (on-the-energy-shell) particles i and j; $\Gamma_{Bb}(E_{Bb})=\sum\limits_{S_fl_f}\Gamma_{Bb_{(S_fl_f)}}(E_{Bb})$ and $\Gamma_{Ax}(E_{Ax})=\sum\limits_{S_il_i}\Gamma_{Ax_{(S_il_i)}}(E_{Ax})$, $\Gamma_{Bb(S_fl_f)}(E_{Bb})$ and $\Gamma_{Ax(S_il_i)}(E_{Ax})$ are the observable partial widths in the final channel $(B+b)_{(S_fl_f)}$ and the initial channel $(A+x)_{(S_il_i)}$.

For the resonant reaction the energy conservation is $E_{Ax}+Q_2=E_{Bb}$, where $Q_2=m_A+m_x-m_B-m_b$, and $E_{R_{Ax}}+Q_2=E_R$, where $E_{R_{Ax}}$ is the resonance energy in the channel $A+x$. Also $\delta_{S_fl_f}$ is the nonresonant scattering phase shift of the fragments B and b in the channel with given S_f and l_f; $Y_{l_fm_{l_f}}(\hat{\mathbf{k}}_{\mathbf{Bb}})$ is the spherical harmonics and $\hat{\mathbf{k}}=\mathbf{k}/k$. $M_{M_yM_F;M_AM_a}$ is the exact amplitude of the direct transfer reaction $a+A\to y+F$ populating the resonance state $F=A+x=B+b$.

The triple differential cross section of TH reaction in the reaction c.m. is given by [6]

$$\frac{\mathrm{d}^3\sigma^{TH}}{\mathrm{d}\Omega_{\hat{\mathbf{k}}_{yF}}\,\mathrm{d}\Omega_{\hat{\mathbf{k}}_{Bb}}\,\mathrm{d}E_{yF}} = \frac{\mu_{Bb}\,\mu_{yF}\,\mu_{Aa}}{2\pi^5}\,\frac{k_{Bb}\,k_{yF}}{k_{Aa}}\,\frac{1}{\hat{J}_a\,\hat{J}_A}\sum_{M_y\,M_B\,M_b\,M_A\,M_a}|M^{TH}_{M_A\,M_a;M_y\,M_B\,M_b}(\mathbf{k}_{yF},\mathbf{k}_{Bb},\mathbf{k}_{Aa})|^2. \tag{8}$$

Inserting Eqs. (6) and (7), integrating Eq. (8) over $\mathrm{d}\Omega_{\hat{\mathbf{k}}_{Bb}}$ and using the orthogonality properties of the spherical functions and the Clebsch-Gordan coefficients, we obtain the TH double differential cross section

$$\frac{\mathrm{d}^2\sigma^{TH}}{\mathrm{d}\Omega_{\hat{\mathbf{k}}_{yF}}\,\mathrm{d}E_{yF}} = \frac{1}{2\pi}\,\frac{\Gamma_{Bb}\,(E_{Bb})}{(E_{Bb}-E_R)^2+\frac{1}{4}\Gamma^2(E_{Bb})} \times\frac{\mathrm{d}\sigma_{(A(a,y)F)}}{\mathrm{d}\Omega_{yF}}. \tag{9}$$

Here $\mathrm{d}\sigma_{(A(a,y)F)}/\mathrm{d}\Omega_{\hat{\mathbf{k}}_{yF}}$ is the differential cross section for the stripping $A(a,y)F$ to the resonant state

$$\frac{\mathrm{d}\sigma_{(A(a,y)F)}}{\mathrm{d}\Omega_{\hat{\mathbf{k}}_{yF}}} = \frac{\mu_{yF}\,\mu_{Aa}}{4\,\pi^2}\,\frac{k_{yF}}{k_{Aa}}\,\frac{1}{\hat{J}_A\,\hat{J}_a} \times\sum_{M_F\,M_y\,M_A\,M_a}|M_{M_F\,M_y;M_A\,M_a}(\mathbf{k}_{yF},\mathbf{k}_{Aa})|^2. \tag{10}$$

Eq. (9) is the basic one and all the other equations can be obtained from it. This equation explains the advantage of the THM for resonant reactions. Comparing the TH double differential cross section, Eq. (9), with the binary resonant cross section (5) we can see that the presence of $\frac{\mathrm{d}\sigma_{(A(a,y)F)}}{\mathrm{d}\Omega_{\hat{\mathbf{k}}_{yF}}}$ rather then the resonance width in the entry channel $\Gamma_{Ax}(E_{Ax})$, which is exponentially small for $E_{xA}\to 0$, makes the TH cross section non-vanishing at astrophysically relevant energies.

The only, but crucial, difference is that the former contains $\frac{\mathrm{d}\sigma_{(A(a,y)F)}}{\mathrm{d}\Omega_{\hat{\mathbf{k}}_{yF}}}$ rather than the entry width $\Gamma_{Ax}(E_{Ax})$. To avoid the impact of the $A-a$ Coulomb barrier on the transfer reaction cross section in the THM the energy E_{Aa} in the entry channel of the TH reaction is chosen to be above the Coulomb barrier, i.e. $\frac{\mathrm{d}\sigma_{(A(a,y)F)}}{\mathrm{d}\Omega_{\hat{\mathbf{k}}_{yF}}}$ is not small making it possible to measure the TH reaction cross section at any small E_{Ax} including $E_{Ax}=0$ and even $E_{Ax}<0$. In the THM the absolute cross sections are not measured and the free resonant cross section can be obtained by normalization of the TH cross section to the available direct measurements at higher energies assuming that $\Gamma_{Ax}(E_{R_{Ax}})$ is known. Such normalization, given by

$$\sigma^R_{(A(x,b)B)} = \frac{\mathrm{d}^2\sigma^{TH}}{\mathrm{d}\Omega_{\hat{\mathbf{k}}_{yF}}\,\mathrm{d}E_{yF}}\,\frac{\Gamma_{Ax}(E_{Ax})}{\frac{\mathrm{d}\sigma_{(A(a,y)F)}}{\mathrm{d}\Omega_{\hat{\mathbf{k}}_{yF}}}}\,\frac{2\,\pi^2}{k^2_{Ax}}\,\frac{\hat{J}_F}{\hat{J}_A\,\hat{J}_x}, \tag{11}$$

provides the resonant cross section down to astrophysically relevant energies where direct data are not available or, if available, may be distorted by the electron screening. We note that Eq. (11) is the extension of the PWIA by taking into account the rescattering of the nuclei in the initial and final states of the transfer reaction $A(a,y)F$. The momentum distribution of the spectator is given by $\frac{\mathrm{d}\sigma_{(A(a,y)F)}}{\mathrm{d}\Omega_{\hat{\mathbf{k}}_{yF}}}$.

Another possibility to use the TH data to determine the resonance cross section is the presence of two isolated resonances, when only one of them is known from direct measurements [5]. In this case, by comparing the TH cross sections of two resonances at resonance energies one can deduce the strength of the unknown resonance. Since the TH data are obtained with a finite energy resolution, which can be significantly larger than the resonance width in the astrophysically relevant energy region, the energy resolution should be taken into account when determining the TH cross section at the resonance energy. The finite experimental energy resolution can be taken into account by

folding the TH double differential cross section with, for example, the Gaussian function whose width is fixed by the energy resolution (assuming that the experimental energy resolution ΔE_{Bb} is greater than the total resonance width $\Gamma(E_R)$) :

$$\frac{d^2\sigma^{TH}}{dE_{yF}\,d\Omega_{\hat{\mathbf{k}}_{yF}}} = \frac{1}{2\pi}\int_{E_R-\Delta E_{Bb}}^{E_R+\Delta E_{Bb}} dx \exp\left[-\frac{1}{2}\left(\frac{x-E_{Bb}}{\sigma}\right)^2\right] \frac{\Gamma_{Bb}(x)}{(x-E_R)^2+\Gamma^2(x)/4} \times\frac{\mathrm{d}\sigma_{(A(a,y)F)}}{\mathrm{d}\Omega_{\hat{\mathbf{k}}_{yF}}}. \quad (12)$$

For a narrow resonance we get

$$\frac{d^2\sigma^{TH}}{dE_{Bb}\,d\Omega_{\hat{\mathbf{k}}_{yF}}} = \frac{\Gamma_{Bb}(E_R)}{\Gamma(E_R)} \times\frac{\mathrm{d}\sigma_{(A(a,y)F)}}{\mathrm{d}\Omega_y}\ \exp\left[-\frac{1}{2}\left(\frac{E_{Bb}-E_R}{\sigma}\right)^2\right]. \quad (13)$$

Assume that there are two isolated resonances and one of them is known. Then the ratio of the TH experimental peaks at resonance energies is

$$\frac{\mathrm{d}\sigma_{(A(a,y)F_1)}(E_{R_1})}{\mathrm{d}\sigma_{(A(a,y)F_2)}(E_{R_2})}\frac{\Gamma_{Bb}(E_{R_1})}{\Gamma(E_{R_1})}\frac{\Gamma(E_{R_2})}{\Gamma_{Bb}(E_{R_2})} = \frac{N_1}{N_2}, \quad (14)$$

where the right-hand-side is the ratio of the TH cross sections at the resonance peaks. Note that in the THM only the relative cross sections are measured.

Eq. (14) allows one to determine the resonance strength of the unknown resonance from the TH measurements if the strength of one of the resonances is known [5]. The resonance strength is given by

$$(\omega\gamma) = \frac{\hat{J}_F}{\hat{J}_x\hat{J}_A}\frac{\Gamma_{Ax}(E_R)\,\Gamma_{Bb}(E_R)}{\Gamma(E_R)}, \quad (15)$$

where the first fraction on the right-hand-side is the statistical factor ω. Then from Eq. (14) we can express the unknown resonance strength in terms of the known one:

$$(\omega\gamma)_1 = \frac{N_1}{N_2}\frac{\mathrm{d}\sigma_{(A(a,y)F_2)}(E_{R_2})}{\mathrm{d}\sigma_{(A(a,y)F_1)}(E_{R_1})}\frac{\Gamma_{Ax}(E_{R_1})}{\Gamma_{Ax}(E_{R_2})}(\omega\gamma)_2\frac{\hat{J}_{F_1}}{\hat{J}_{F_2}}. \quad (16)$$

3 Two interfering resonances. Two-level, two-channel case

Consider now the two-level, two-channel case. The THM reaction amplitude in the presence of two interfering resonances in the compound nucleus F takes the form (if nuclear spins are neglected) [7]

$$M^{(TH)} = \sum_{\tau,\nu=1,2}\Gamma^{1/2}_{bB(\tau)}(E_{bB})\,[\mathbf{L}^{-1}]_{\tau\nu}M_\nu(\mathbf{k}_{yF},\mathbf{k}_{aA}), \quad (17)$$

where $\mathbf{L}$ is the level matrix, $\Gamma_{ij(\tau)}(E_{ij})$ is the partial width of resonance τ in the channel $i+j$, M_τ is the amplitude for the direct transfer reaction $x+A\to y+F_\tau$ populating the compound state F_τ of the system $F=A+a=B+b$. It is a general expression for the double differential cross section for the TH reaction (2), which proceeds through the subreaction (1) contributed by interfering resonances. Eq. (17) is generalization of the two-level, two-channel R matrix amplitude for the TH reaction.

Correspondingly the double TH differential cross section is given by

$$\frac{d^2\sigma^{TH}}{dE_{yF}\,d\Omega_{\hat{\mathbf{k}}_{yF}}} = \frac{1}{2\pi}\frac{d\sigma_{A(a,y)F_1}}{d\Omega_{\mathbf{k}_{yF}}} \times\Big|\sum_{\tau,\nu=1,2}\Gamma^{1/2}_{bB(\tau)}(E_{bB})[L^{-1}]_{\tau\nu}\,R_\nu\Big|^2, \quad (18)$$

$$R_\nu(\mathbf{k}_{yF},\mathbf{k}_{aA}) = \frac{M_\nu(\mathbf{k}_{yF},\mathbf{k}_{aA})}{M_1(\mathbf{k}_{yF},\mathbf{k}_{aA})}. \quad (19)$$

To derive Eq. (18) we took out from the sum amplitude $M_1(\mathbf{k}_{yF},\mathbf{k}_{aA})$ for the transfer reaction $A(a,y)F_1$ populating the first resonance.

4 Application of the TH for analysis of the CNO cycle reaction $^{15}\mathrm{N}(p,\alpha)^{12}\mathrm{C}$

^{15}N(p,α)^{12}C is an important CNO cycle reaction and plays a crucial role in the production chain of the key isotope ^{19}F in AGB stars. Because of its astrophysical relevance (see [8] and reference therein) it has been subject to both direct [9–11] and indirect (via the Trojan Horse method (THM)) [8] investigations to extend our knowledge down to the Gamow window. A recent R matrix fit to the direct measurements of this reaction by Zyskind and Parker [9] and Redder [11] was presented in [12]. In these fits two different sets of data from [11] were used: one that included the full 71 data points (R71), and one that used the lowest energy data (R32). The R matrix fit in [12] to the direct data yields $S(0)\approx 80$ MeVb, which is considerably above the values recommended by all other publications except for the result from [9], which has a 15% systematic and 8% statistical uncertainty.

Moreover, the reliability of the THM data was questioned in [12]. The ^{15}N(p,α)^{12}C reaction is contributed by two interfering 1^- resonances in ^{16}O at 312 and 960 keV. In [8] the astrophysical $S(E)$ factor for this reaction was obtained using the TH reaction $^{15}\mathrm{N}(d,n\alpha)^{12}\mathrm{C}$.

New calculations shown in Fig. 1 present compelling evidence that the THM measures the same cross section as the direct measurements [13] . The smearing over the

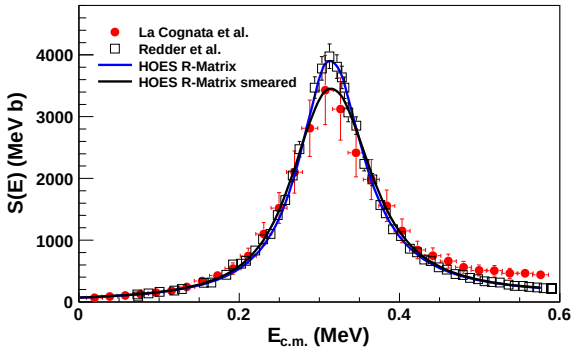

Fig. 1. (Color online) Black solid line is a 20 keV energy resolution folded R matrix fit to THM data (red dots)[8], giving $S(0) = 70 \pm 8$ MeVb ($\chi^2/N = 1.16$) . The parameters of the fit are given in [13]. The blue solid line is the R matrix fit of the R32 data ($\chi^2/N = 1.39$) obtained with the same parameters as the solid black line. For comparison, the $S(E)$ factor from Ref. [11] is given as open squares.

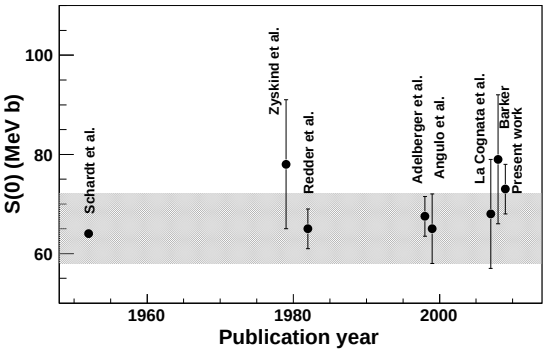

Fig. 2. Summary of the available astrophysical $S(0)$ factors of the ^{15}N(p,α)^{12}C reaction.

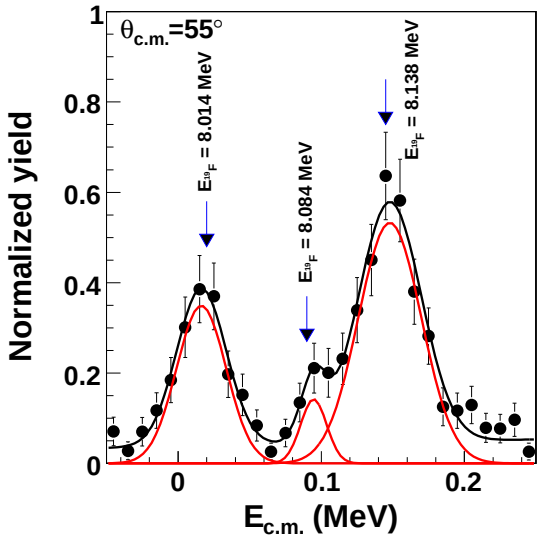

Fig. 3. (Color online) The TH excitation function (in arbitrary units) for the ^{18}O$(p,\alpha)^{15}$N reaction obtained for a fixed scattering angle $\theta_{c.m.} = 55°$, in the 0 – 250 keV energy range. A Gaussian fit (red lines) is used to disentangle the contribution of each peak to the overall normalized coincidence yield. The black solid line is the sum of the obtained Gaussian functions and of a straight line to provide for the nonresonant contribution.

energy resolution affects only the maximum value of the resonance peak keeping the resonance area the same and does not affect the low-energy tail. This effect was not included in the analysis carried out in Ref. [12], which led to a different result quoted there. The $S(E)$ factor folded with 20 keV energy-resolution and obtained using Eq. (12) (the black solid line in Fig. 1), where Eq. (18) is used for the TH double differential cross section with the infinite resolution, is in a perfect agreement with our THM data. The total uncertainty of the TH data is 16% [8]. An additional 11% comes from the uncertainty of the ratio of the direct transfer amplitudes corresponding to the population of the resonances at 312 and 960 keV, which is caused by the transfer reaction experimental uncertainties not related to the TH reaction. Then the total uncertainty of the TH $S(E)$ factor we estimate to be 19%. Thus we get from the THM $S(0) = 70.0 \pm 13.5$ MeVb factor, which agrees with the direct R71 and R32 data fits. A significant part of the χ^2 for the THM data fit comes from the energy region $E > 400$ keV, where the contribution from the non-THM mechanism, sequential decay of ^{13}C, becomes significant. We have verified that the modified R matrix approach correctly describes the THM $S(E)$ factor in the case of resonant reactions. This provides, on one hand, an explanation of why the THM is working and, on the other, allows one to deduce a reliable $S(0)$ factor for astrophysical application.

Fig. 2 demonstrates that all the experimental values are in agreement with each other within the experimental uncertainties, resulting in $S(0) \approx 62$ [10], $S(0) = 78 \pm 13$ [9], $S(0) = 65 \pm 4.0$ [11], and $S(0) = 68 \pm 11$ MeV b [8]. The compilations by NACRE [14] and Adelberger et al. [15] recommended $S(0) = 65 \pm 7$ and $S(0) = 67.5 \pm 4.0$ MeV b, correspondingly, relying on the results from Ref. [11].

5 Reaction ^{18}O$(p,\alpha)^{15}$N via the THM

The knowledge of the reaction rates for the ^{18}O$(p,\alpha)^{15}$N reaction can help to pin down the uncertainties, due to nuclear physics input, affecting present-day models of asymptotic giant branch stars. Its reaction rates can modify both fluorine nucleosynthesis inside such stars as well as oxygen and nitrogen isotopic ratios, which allow one to constrain the proposed astrophysical scenarios. This reaction is contributed by low-energy resonances at 20, 90, 144 keV and two higher energy resonances. Due to the very small penetration factor in the entry channel ^{18}O + p it is practically impossible to observe directly the two lowest resonances. That is why the THM is the only method which allows one to observe the low-energy resonances at 20 and 90 keV and determine their contribution to the reaction rates. To determine the reaction rates for the ^{18}O$(p,\alpha)^{15}$N reaction the TH reaction ^{18}O$(d,n\alpha)^{15}$N was used [5] The low-energy TH spectrum is shown in Fig. 3.

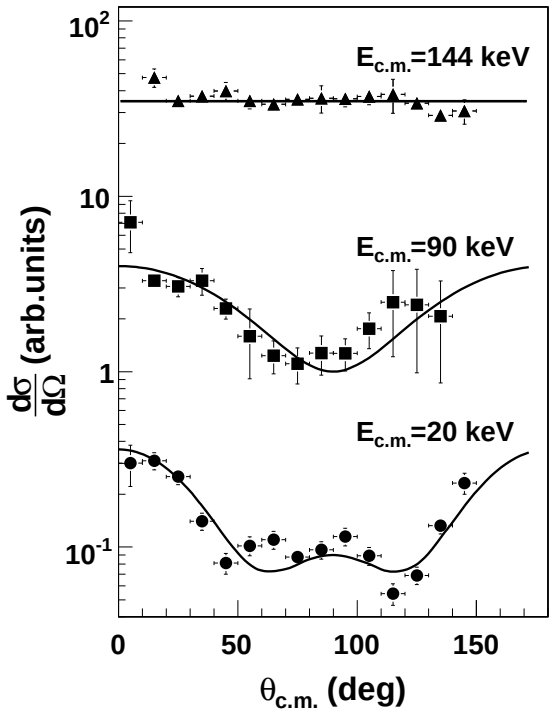

Fig. 4. Experimental angular distributions for the $^{18}O(p,\alpha)^{15}N$ reaction for the three resonances in the 0 - 250 keV energy range. The full lines are the theoretical angular distributions for the free $^{18}O(p,\alpha)^{15}N$ reaction, calculated using the equations from [16].

Only using the THM we could observe the low-energy resonances. Note that the partial widths of the resonances are very small and the observed broadening of the widths in Fig. 3 is due to the experimental energy resolution.

We find that the momentum distribution given by the Fourier transform of the deuteron bound state wave function is very close to the one given by the DWBA transfer cross section at $p_{np} < 40$ MeV/c. To test the THM in Fig. 4 we compare the measured from the TH reaction angular distributions of the fragments $\alpha - {}^{15}N$ with the calculated one for the binary reaction $^{18}O(p,\alpha)^{15}N$ proceeding through the three low-lying resonances.

For the resonance at 144 keV the THM data confirm the assignment $J^\pi_F = \frac{1}{2}^+$, $l_i = 0$ and $l_f = 1$, where l_i and l_f are the orbital angular momenta in the initial and final states of the resonant reaction. Assuming that the spin-parity assignments in [5] is correct, we have calculated the angular behavior of the differential cross sections for the resonances at 20 and 90 keV. Agreement of these calculations with the experimental angular distributions determined from the TH reaction confirmed the validity of the assignments in [5]: $J^\pi_F = \frac{5}{2}^+$, $l_i = 2$ and $l_f = 3$ for the resonace at 20 keV and $J^\pi_F = \frac{3}{2}^+$, $l_i = 2$ and $l_f = 1$ for the 90 keV resonance.

In [5] using Eq. (16) the resonance strengths for the 20 and 90 keV resonances were determined and the reaction rates for the $^{18}O(p,\alpha)^{15}N$ reaction were calculated.

This work was supported by the U. S. Department of Energy under Grant No. DE-FG02-93ER40773, DE-FG52-06NA26207 and NSF Grant No. PHY-0852653.

References

1. G. Baur, Phys. Lett. **B 178**, (1986) 135.
2. C. Spitaleri *et al.*, Phys. Rev. **C 60**, (1999) 055802.
3. R. G. Pizzone *et al.*, Phys. Rev. **C 80**, (2009) 025807.
4. C. Spitaleri *et al.*, Phys. Rev. **C 69**, (2004) 055806.
5. M. La Cognata *et al.*, Phys. Rev. Lett. **101**, (2008) 152501.
6. E. I. Dolinsky *et al.*, Nucl. Phys. **A202**, (1973) 97.
7. A. M. Mukhamedzhanov *et al.*, J. Phys. G: Nucl. Part. Phys. **35**, (2008) 014016.
8. M. La Cognata *et al.*, Phys. Rev. **C 76**, (2007) 065804.
9. J.L. Zyskind & P.D. Parker, Nucl. Phys. **A320**, (1979) 404.
10. A. Schardt *et al.*, Phys. Rev. **86**, (1952) 527.
11. A. Redder *et al.*, Z. Phys. **A305**, (1982) 325.
12. F.C. Barker, Phys. Rev. C **78**, (2008) 044611.
13. M. La Cognata *et al.*, Phys. Rev. **C 80**, (2009) 012801(R).
14. C. Angulo *et al.*, Nucl. Phys. **A656**, (1999) 3.
15. E.G. Adelberger *et al.*, Rev. Mod. Phys. **70**, (1998) 1265.
16. J. M. Blatt and L. C. Biedenharn, Rev. Mod. Phys., **24**, (1952) 258.